Embedded Wavelet Coding of Arbitrarily Shaped Objects

Alfred Mertins and Sudhir Singh

University of Wollongong
School of Electrical, Computer and Telecommunications Engineering
Wollongong NSW 2522, Australia

ABSTRACT

This paper presents an embedded zerotree wavelet coding technique for the compression of arbitrarily shaped 2-D objects. The wavelet decomposition is carried out with an optimized, biorthogonal, shape adaptive discrete wavelet transform (SA DWT) which performs non-expansive multiresolution decompositions of arbitrary image regions. The proposed SA DWT is defined for even-length, symmetric wavelet filters such as the 6-10 filters. The processing at region boundaries is carried out via reflection, followed by an optimization stage which requires only a few operations per boundary pixel. The computationally inexpensive optimization results in an additional performance gain of up to 0.5 dB compared to the plain reflection based scheme.

Keywords: Shape adaptive wavelet transform, region based coding, object based coding, embedded zerotree coding, non-expansive transform

1. INTRODUCTION

Shape-adaptive (SA) transforms are of significant importance for object-based image and video coding, because many upcoming multimedia applications require object-based rather than frame-based data access. Since the objects describing a scene may occur with any shape, the transforms used for compression need to be able to operate on arbitrarily shaped regions of support. Several concepts are known for this purpose. In Ref. 1 a polynomial-based method was proposed. In this approach, the set of basis vectors is generated according to the given object shape, and the basis globally depends on the object shape. A simple, powerful, and computationally efficient technique is the shape adaptive DCT,[2] which has been proposed for the emerging MPEG-4 standard.[3] In this approach, the interior region of an object is transformed by using the standard 2-D DCT, while the boundary regions are processed in a shape adaptive manner. As with all DCT-based approaches, the occurrence of blocking artifacts at very low rates is one of the major drawbacks. A promising alternative is the discrete wavelet transform (DWT), which is generally known for its excellent coding properties without blocking artifacts. Shape adaptive versions of the DWT have been proposed in Refs. 3–8. The ones in Refs. 3–7 are based on support preservative 1-D decompositions of rows and columns of 2-D objects. All of them use linear-phase filters and employ reflection techniques at the boundaries to achieve support preservation. The method in Ref. 8 introduces redundancy.

In this paper, we consider support preservative SA DWTs based on 1-D transforms. In particular, we look at schemes for even-length analysis and synthesis filters, such as the 6-10 filters of Ref. 9. The basic scheme proposed in this paper considers symmetric reflection at the region boundaries. Based on this scheme, it will be shown that the performance can be enhanced by including a simple optimization step. This optimization is related to the boundary filter optimization in Ref. 10. However, the computational cost of the proposed optimization is much lower than in Ref. 10. It amounts, on average, to a single multiplication per boundary pixel. The rate-distortion performance of the proposed scheme will be compared to the MPEG-4 scheme in Ref. 3, which uses odd-length filters. For all decomposition schemes, a dedicated, shape adaptive, embedded zerotree coder is used.

The paper is organized as follows. In Section 2, we outline the SA DWTs used in MPEG-4[3] and the one proposed in this paper. Section 3 outlines the optimization step in the proposed approach. In Section 4, we discuss the embedded, shape adaptive, zerotree coder. Section 5 presents coding results and Section 6 gives some conclusions.

Correspondence: A. Mertins, University of Wollongong, School of Elec., Comp., Tele. Engg., Wollongong NSW 2522, Australia. Telephone +61 2 4221-3410, Facsimile +61 2 4221-3236, E-mail: alfred.mertins@ieee.org

2. SHAPE ADAPTIVE WAVELET TRANSFORMS

We consider shape adaptive wavelet transforms based on separate 1-D decompositions.[3–7] Since we are interested in object-based compression, and because the objects describing a scene may occur with any shape, it is desirable to have SA DWTs which yield non-expansive subband decompositions for arbitrarily shaped regions of support while maintaining a high compaction gain and allowing perfect reconstruction. A non-expansive transform is one where the total number of transform coefficients is equal to the total number of input samples. This property can be achieved by using appropriate boundary processing schemes.[10–17] Note that some of these schemes are only applicable to certain signal length, for example even length, or lengths which are an integer multiple of the number of subbands. To operate on arbitrarily shaped regions of support, it is necessary to achieve the above mentioned properties for arbitrary signal lengths.

A particular problem in 2-D shape adaptive wavelet transforms is that the decomposition in one dimension should introduce a minimum amount of distortion in the second dimension. For the interior of a region this can be accomplished by using different subsampling phases for rows (columns) that start at even or odd positions.[10] Of course, the regions need to be large enough to ensure that the processing of the interior is not influenced by the shape of the region. In the boundary regions themselves, the distortion depends on the outline of the region and the boundary processing. In the following two subsections, we will discuss two schemes which allow for ideal processing of the interior of an object, while maintaining good properties at the boundaries. The first one has been proposed for MPEG-4[3] and considers odd-length, linear phase filters with unequal length for the low and highpass, such as the 9-7 filters. The second one is the scheme proposed in this paper. This scheme is designed for even-length, linear phase filters, such as the 6-10 filters.

2.1. A Scheme for Odd-length, Linear Phase Filters

With odd-length, biorthogonal, linear phase filters, a non-expansive transform is easily achieved by using symmetric reflection at the boundaries. The reflection principle works for arbitrary signal length. Figure 1 depicts the processing schemes for the four cases of interest: (a) even-length signal starting at an even position*; (b) even-length signal starting at an odd position; (c) odd-length signal starting at an even position; (d) odd-length signal starting at an odd position. The upper rows in Figs. 1(a)-(d) show the extended input signal, where the given input samples are surrounded by solid boxes. The lowpass and highpass subband samples, c_n and d_n, respectively, are computed by taking the inner products of the impulse responses in the displayed positions with the corresponding part of the extended input signal. As the figures show, only the desired number of different lowpass and highpass coefficients occurs and has to be transmitted. To reconstruct a signal from its subband samples, the subband signals have to be extended at their boundaries according to the symmetries for the given case and then fed into the synthesis filters.

The decomposition scheme in Fig. 1 can be used for all signal length being larger than one. For the treatment of single samples, different strategies have been proposed. The methods in Refs. 13,4,10,18 distinguish between pixels being located at even and odd positions: If a single sample occurs at an even position, it is multiplied with the DC amplification of the analysis lowpass and copied into the lowpass band at the appropriate position. If it occurs at an odd position it is copied into the highpass band and marked as a special sample. This treatment of single samples has the advantage that the region-based DWTs of all segments of a segmented image can be stored in a single matrix, just like the DWT of an entire frame. No conflicts occur with transform coefficients from different segments that might need to be stored at the same location. These decomposition schemes even allow for edge-based DWTs such as the one in Ref. 18. The region-based DWT proposed for the upcoming multimedia standard MPEG-4[3] is different in its treatment of length-one signals. In this approach, independent of the position of a single sample, the sample is multiplied with the DC amplification of the analysis lowpass and copied into the lowpass band. This can be done because the philosophy in MPEG-4 is to have a set of objects which describe a scene, but the objects do not necessarily have to be non-overlapping segments of a single frame. Consequently, there is no need to ensure that the transform coefficients can be stored in specific locations within the decomposed image, as it would be the case for the edge-based coding method in Ref. 18.

Figure 2 further illustrates the wavelet decomposition of arbitrarily shaped objects in MPEG-4. The processing is based on the schemes in Fig. 1. The single pixels at even and odd positions in Fig. 2(a) result in pixels in the lowpass band in Fig. 2(b). The final four-band decomposition is depicted in Fig. 2(c). Note that it is not possible to

*We distinguish between segments that start or stop at even or odd positions. The pixel in the upper left corner of an image is said to be at position (0,0).

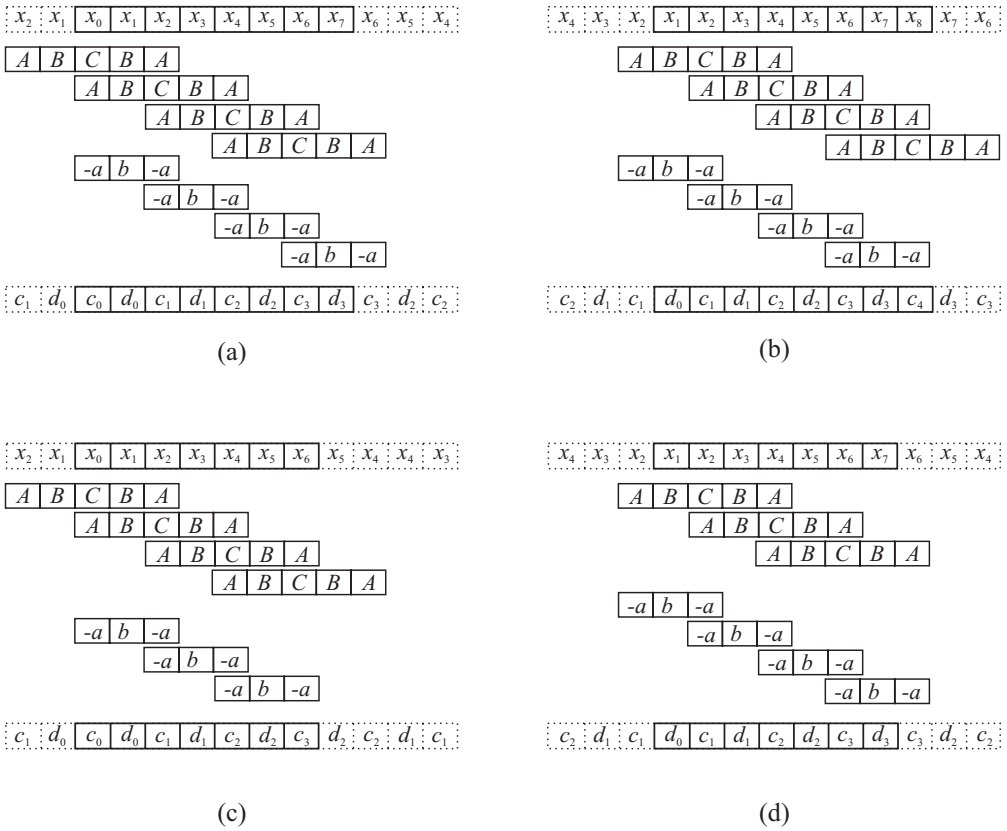

Figure 1. Symmetric reflection using odd-length symmetric filters with impulse responses $\{A, B, C, B, A\}$ for the lowpass and $\{-a, b, -a\}$ for the highpass; (a) even-length signal starting at an even position; (b) even-length signal starting at an odd position; (c) odd-length signal starting at an even position; (d) odd-length signal starting at an odd position.

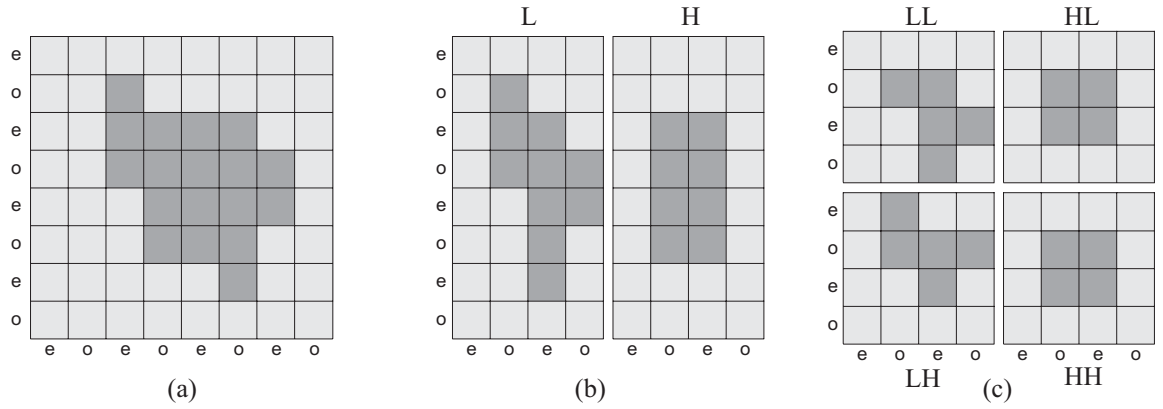

Figure 2. Decomposition of a non-rectangular object with odd-length, linear-phase filters according to MPEG-4; (a) the object, shown in dark gray; (b) the decomposed object after horizontal filtering; (c) decomposed object after vertical filtering. The letters "e" and "o" indicate the position (even or odd) of a pixel in the horizontal and vertical dimensions.

process also the exterior of the object in Fig. 2(a) and store the resulting wavelet coefficients in the exterior of the decomposed object in Fig. 2(c) in the usual manner, because the space occupied by the single pixel in the second last row would be required twice. Following the MPEG-4 philosophy, this is not a drawback. An advantage of the

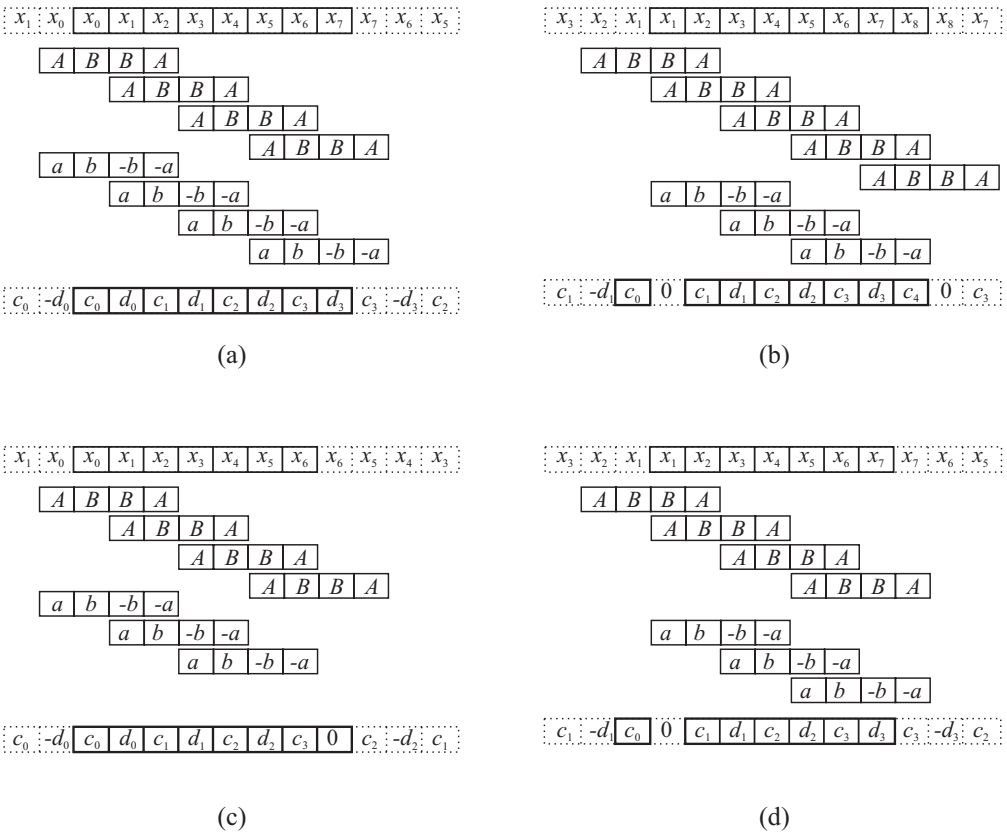

Figure 3. Symmetric reflection for even-length, linear-phase filters with impulse responses $\{A, B, B, A\}$ for the lowpass and $\{-a, -b, b, a\}$ for the highpass; (a) even-length signal starting at an even position; (b) even-length signal starting at an odd position. (c) odd-length signal starting at an even position; (d) odd-length signal starting at an odd position.

scheme is that an object containing a constant dc value will result in a decomposed image where a constant value occurs in the LL band, while all other bands contain zeros.

2.2. The proposed scheme for Even-length, Linear Phase Filters

The proposed scheme for even-length, linear phase filters involves symmetric reflection at the boundaries, just like the one in Section 2.1. However, for even-length filters a different type of symmetry is used. The schemes for the four cases of interest are depicted in Fig. 3. In Fig. 3(a) an even-length signal which starts at an even position is decomposed into an equal number of lowpass and highpass coefficients. This scheme is usually applied when an entire frame is transformed with a DWT based on even-length, linear phase filters. The processing of an even length segment starting at an odd position is shown in Fig. 3(b). In this case, two highpass coefficients, one at the beginning and one at the end, occur, which are identically zero and do not need to be transmitted. This compensates for the increased number of lowpass coefficients, and in total a non-expansive transform is achieved. The schemes in Figs. 3(c) and (d) are combinations of the ones in Figs. 3(a) and (b). For segments of length two which start at an odd position, an exemption from the scheme in Fig. 3 is introduced. In this case, the scheme in Fig. 3(a) is used instead of the one in Fig. 3(b), because otherwise no effective filtering operation would be carried out.

The wavelet decomposition of a non-rectangular object using the schemes in Fig. 3 and the one exemption made, is illustrated in Fig. 4. As with the MPEG scheme, an object containing a constant value will result in a decomposed image where a constant value occurs in the LL band, while all other bands contain zeros. Also, it is easily verified that it is not possible to process the exterior of the object and store the resulting wavelet coefficients in the exterior of the decomposed object in Fig. 4(c), because problems with double occupations occur. For the MPEG-4 concept of objects this is no drawback.

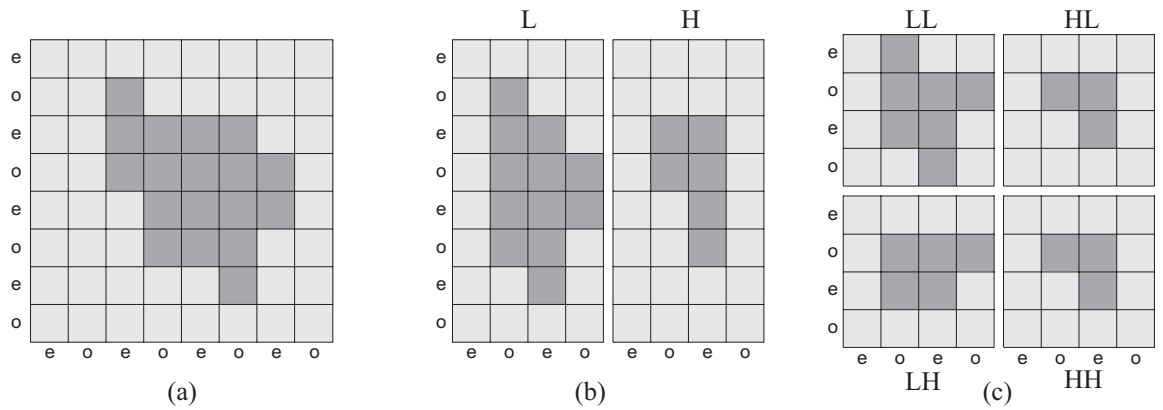

Figure 4. Decomposition of a non-rectangular object with even-length, linear-phase filters; (a) the object, shown in dark gray; (b) the decomposed object after horizontal filtering; (c) decomposed object after vertical filtering. The letters "e" and "o" indicate the position (even or odd) of a pixel in the horizontal and vertical dimensions.

$$\left[\begin{array}{cccccccc}
h_{\ell_0}(2) & h_{\ell_0}(1) & h_{\ell_0}(0) & & & & & \\
h_{\ell_1}(2) & h_{\ell_1}(1) & h_{\ell_1}(0) & & & & & \\
\hline
h_0(3) & h_0(2) & h_0(1) & h_0(0) & & & & \\
h_1(3) & h_1(2) & h_1(1) & h_1(0) & & & & \\
 & & h_0(3) & h_0(2) & h_0(1) & h_0(0) & & \\
 & & h_1(3) & h_1(2) & h_1(1) & h_1(0) & & \\
\hline
 & & & & & & h_{r_0}(3) & h_{r_0}(2) h_{r_0}(1) \\
 & & & & & & h_{r_1}(3) & h_{r_1}(2) h_{r_1}(1)
\end{array}\right]$$

(a)

$$\left[\begin{array}{cc|cccc|cc}
g_{\ell_0}(1) & g_{\ell_1}(1) & & & & & & \\
g_{\ell_0}(2) & g_{\ell_1}(2) & g_0(0) & g_1(0) & & & & \\
g_{\ell_0}(3) & g_{\ell_1}(3) & g_0(1) & g_1(1) & & & & \\
 & & g_0(2) & g_1(2) & g_0(0) & g_1(0) & & \\
 & & g_0(3) & g_1(3) & g_0(1) & g_1(1) & & \\
 & & & & g_0(2) & g_1(2) & g_{r_0}(0) & g_{r_1}(0) \\
 & & & & g_0(3) & g_1(3) & g_{r_0}(1) & g_{r_1}(1) \\
 & & & & & & g_{r_0}(2) & g_{r_1}(2)
\end{array}\right]$$

(b)

Figure 5. Example of size-limited analysis and synthesis matrices ($N = 8$, length-4 filters, even start position); (a) $\boldsymbol{H}$; (b) $\boldsymbol{G}$.

The fact that the proposed scheme results in an increased number of lowpass coefficients (compared to odd-length filters) might suggest that the compaction gain is somewhat reduced. However, because the decomposition is repeated and typically a five-level decomposition is performed, the opposite is the case. From decomposition level to decomposition level, the shape of the lowpass (LL) band becomes more and more regular than for other SA DWTs, the effects due to irregular shapes decrease, and the compaction gain increases.

3. THE OPTIMIZATION STEP

To outline the optimization step, let us look at the common description of all possible two-band decompositions of a length-N input signal $\boldsymbol{x}$ given by

$$\boldsymbol{y} = \boldsymbol{H}\,\boldsymbol{x} \tag{1}$$

The vector $\boldsymbol{x}$ can be considered as an arbitrary-length segment of a row or column of an image. The vector $\boldsymbol{y}$ contains the subband samples in increasing order (e.g. $\boldsymbol{y}^T = [c_0, d_0, c_1, d_1, \ldots]$ where c_n are the lowpass and d_n are the highpass subband samples). The rows of the $N \times N$ matrix $\boldsymbol{H}$ contain the time-shifted analysis impulse responses in reversed order. The synthesis operation can be written as

$$\hat{\boldsymbol{x}} = \boldsymbol{G}\,\boldsymbol{y}, \tag{2}$$

where the columns of $\boldsymbol{G}$ contain the impulse responses of the synthesis filters. Figure 5 gives an illustration. The first and last rows of $\boldsymbol{H}$, and the first and last columns of $\boldsymbol{G}$ contain the boundary filters whose impulse responses are different from the ones used in steady state. With respect to their position (left or right) they are denoted as

Table 1. Energies of boundary filters for segments starting at even and odd positions, respectively. The filter bank is based on the 6-10 filters.

	even start				odd start			
	1st	2nd	3rd	nominal value	1st	2nd	3rd	nominal value
Analysis lowpass	0.9247	1.0276	1.0276	1.0276	2.0552	1.0177	1.0276	1.0276
Analysis highpass	0.9242	1.0224	1.0276	1.0276	1.0098	1.0273	1.0276	1.0276
Synthesis lowpass	1.1006	1.0051	1.0000	1.0000	0.5000	1.0174	1.0003	1.0000
Synthesis highpass	1.1002	1.0000	1.0000	1.0000	1.0096	1.0000	1.0000	1.0000

Table 2. Energies of modified boundary lowpass filters for segments starting at odd positions ($\alpha = 0.7$).

	even start				odd start			
	1st	2nd	3rd	nominal value	1st	2nd	3rd	nominal value
Analysis lowpass	0.9247	1.0276	1.0276	1.0276	1.0122	1.0177	1.0276	1.0276
Synthesis lowpass	1.1006	1.0051	1.0000	1.0000	1.0204	1.0174	1.0003	1.0000

$h_{l_0}(n), h_{l_1}(n), \ldots, g_{r_0}(n), g_{r_1}(n)$. The matrix $\boldsymbol{H}$ can be constructed such that it exactly produces the same subband samples as the schemes in Figs. 1 and 3, respectively. Similarly, the matrix $\boldsymbol{G}$ can be chosen to describe exactly the same synthesis operation as carried out with the methods described in Section 2. The advantage of the boundary filter interpretation, however, is that it allows us to gain some insight into the properties of the boundary filtering operations.

One problem, which has been addressed in Refs. 19 and 10, is that the boundary filters may have energies that can be significantly different from the energies of the original filters. This may result in visible artifacts due to unequal amplification of quantization noise in the synthesis stage. If the synthesis filters have spatially varying energies, a white quantization noise may result in a colored, spatially varying noise after reconstruction. In Ref. 19, where only 1-D signals were considered, it was proposed to adjust the bit allocation according to the filter energies. In a 2-D setting with arbitrarily shaped objects, however, such a strategy would become extremely difficult, because the energies depend on the actual shape and cannot be pre-computed for all configurations. The method in Ref. 10 solves the problem by optimizing the boundary filters in such a way that all filters almost perfectly have the desired energies while preserving other desired properties like vanishing moments.

We consider optimization only for the even-length 6-10 filters. Table 1 shows the energies of the boundary filters for the even-length 6-10 filters and the processing of the left boundary of a finite-length signal, using the method described in Sect. 2.2. With one exception it turns out that the boundary filters' energies are very close to their nominal values and do not necessarily need adjustment. The exception occurs for the first boundary lowpass for processing segments that start at odd positions. In this case, the analysis filter has twice the nominal energy. The aim is to reduce this value to a value being close to one, while maintaining a constant dc amplification.

Let us consider the processing of a segment $\{x_1, x_2, x_3, \ldots\}$, which starts at an odd position and produces the lowpass values $\{c_0, c_1, c_2, \ldots\}$. The optimization step is to replace the value c_0 by

$$c_0' = \alpha\, c_0 + (1 - \alpha)\, c_1 \tag{3}$$

and to use c_0' instead of c_0 for further processing. On the synthesis side, the value c_0 has the be recovered as

$$c_0 = \alpha^{-1} c_0' + (1 - \alpha^{-1})\, c_1 \tag{4}$$

Note that the above operation does not change the dc amplification of the boundary filters. Table 2 shows the energies of the boundary filters for $\alpha = 0.7$. As we see, the energy of the first boundary analysis lowpass drops from 2.0552 to 1.0122. Accordingly, the energy of the first boundary synthesis lowpass increases from 0.5 to 1.0204. Thus, with $\alpha = 0.7$ a good overall performance is achieved.

The processing of the right-hand side of a segment is similar to the processing on the left-hand one. The optimization is needed for the case where a segment stops at an even position. In this case, the last lowpass value, say c_N, is to be replaced by

$$c'_N = \alpha\, c_N + (1-\alpha)\, c_{N-1} \tag{5}$$

with the same α as before. The inverse operation is required on the synthesis side.

Note: To be able to carry out the aforementioned steps, it is necessary to have at least three samples in the lowpass band.

4. EMBEDDED ZEROTREE CODING

Embedded zerotree coders use the parent-child relationships in the wavelet domain to efficiently encode an image.[20,21] In the case of arbitrarily shaped objects, the problem of disturbed parent-child relationships in the boundary regions arises. Two effects can be observed[7]:

1. The descendants of samples at a higher level may not belong to the object;
2. The parents of some samples may not belong to the object.

To cope with such situations the pixel scanning procedure of the EZW algorithm has to be modified in such a way that only pixels belonging to the object are scanned and coded. When coding insignificant coefficients only descendants that belong to the object need to be used for comparison with the given threshold. The algorithm implemented is based on the EZW algorithm of Ref. 20. However, similar modifications can be done to the one of Ref. 21.

5. RESULTS

We compare the different shape adaptive wavelet transforms presented in the previous sections for two example images. First we consider coding of the foreground of the first frame of the Akiyo sequence (QCIF format). The test image is shown in Fig. 6(a), and its SA DWT is depicted in Fig. 6(b). Rate-distortion (RD) results for coding this image are presented in Fig. 7. The rate is measured in terms of the number of symbols coded by the SA EZW coder, without further entropy coding. As we see, the proposed SA DWTs based on the even-length 6-10 filters outperform the odd-length 9-7 ones for almost all rates. The performance gain of the 6-10 over the 9-7 filters is up to 1 dB for certain rates. Also, the gain due to optimization reaches up to 0.5 dB.

The performance gain of the proposed SA DWT over the MPEG scheme with 9-7 filters can be partly explained by the fact that the proposed SA DWT yields a lower number of subband samples without parents at the next level. A five-level decomposition of the Akiyo image using the MPEG scheme results in 263 pixels without parents. Similar numbers occur for the schemes in Refs. 4–6. The SA DWT proposed in this paper yields only 132 pixels without parents, which allows for a more efficient use of the zerotree concept in boundary regions. Also, the shape of the lowpass (LL) band is more regular than for other SA DWTs. This is not so obvious in the Akiyo example, but it can be seen when looking at more complex shapes.

In a second example, we look at coding the region of the cameraman image being depicted in Fig. 8. The results in Fig. 9 show that for this image the performance gain of the proposed SA DWT over the MPEG one is up to 2 dB. The optimization yields an improvement for most rates, but it may also result in a degradation for some rates. The reason for this is that the thresholds used in the EZW algorithm are different and that the dominant and subordinate passes are carried out after different numbers of encoded symbols, resulting in differently shaped RD curves. For the part of the cameraman image considered in this example, the initial thresholds are 658 for the optimized and 1140 for the non-optimized case.

The fact that the proposed SA DWT produces more regular shapes of the LL bands than other DWTs is demonstrated in Fig. 10.

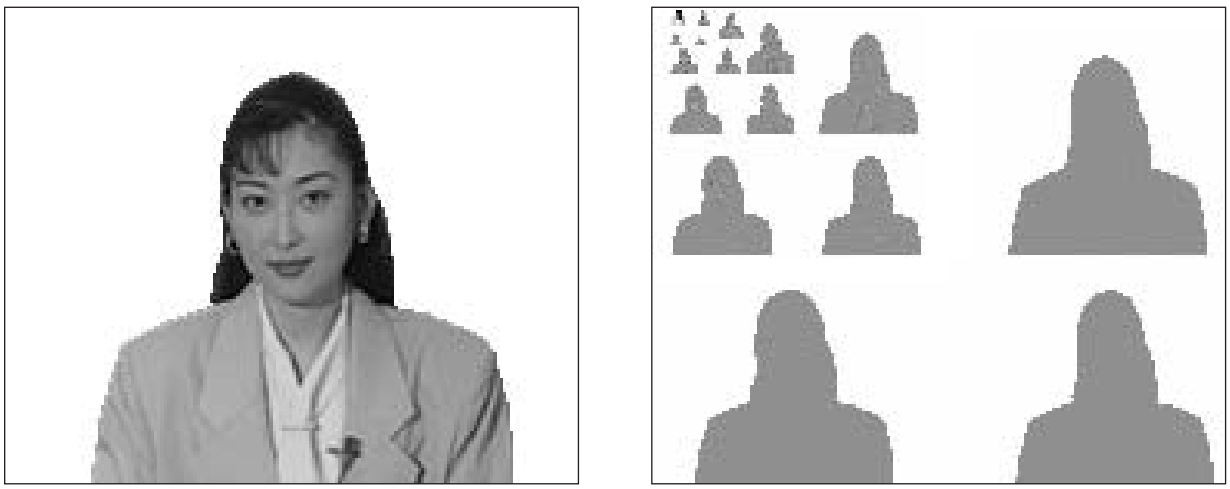

(a) (b)

Figure 6. Akiyo image and its SA DWT; (a) foreground of first frame, QCIF; (b) SA DWT.

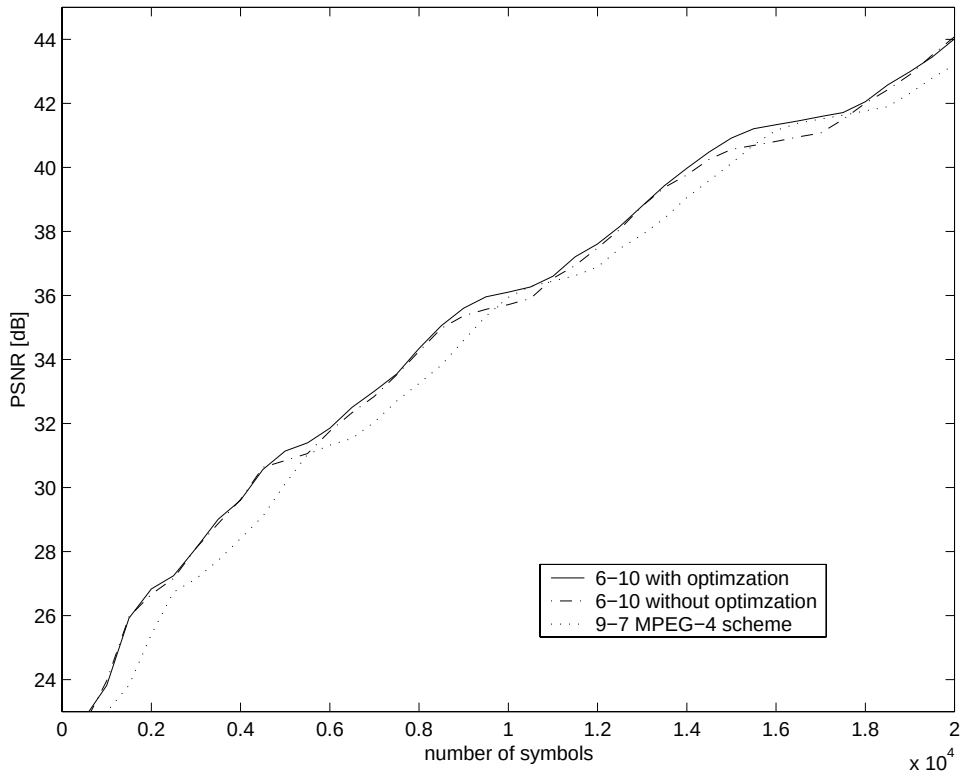

Figure 7. Rate-distortion results for the Akiyo foreground. The rate is measured in terms of the number of symbols coded by the SA EZW coder.

6. CONCLUSIONS

In this paper, a 2-D SA DWT based on even-length filters has been proposed. In this transform, the decomposition typically results in more lowpass samples than with other known approaches. This might suggest that the compaction gain of the proposed transform is lower than for other SA DWTs. However, because the decomposition is repeated and typically a five-level decomposition is performed, the opposite is the case. From decomposition level to decomposition

Figure 8. Region of cameraman image (the full image is of size 256×256).

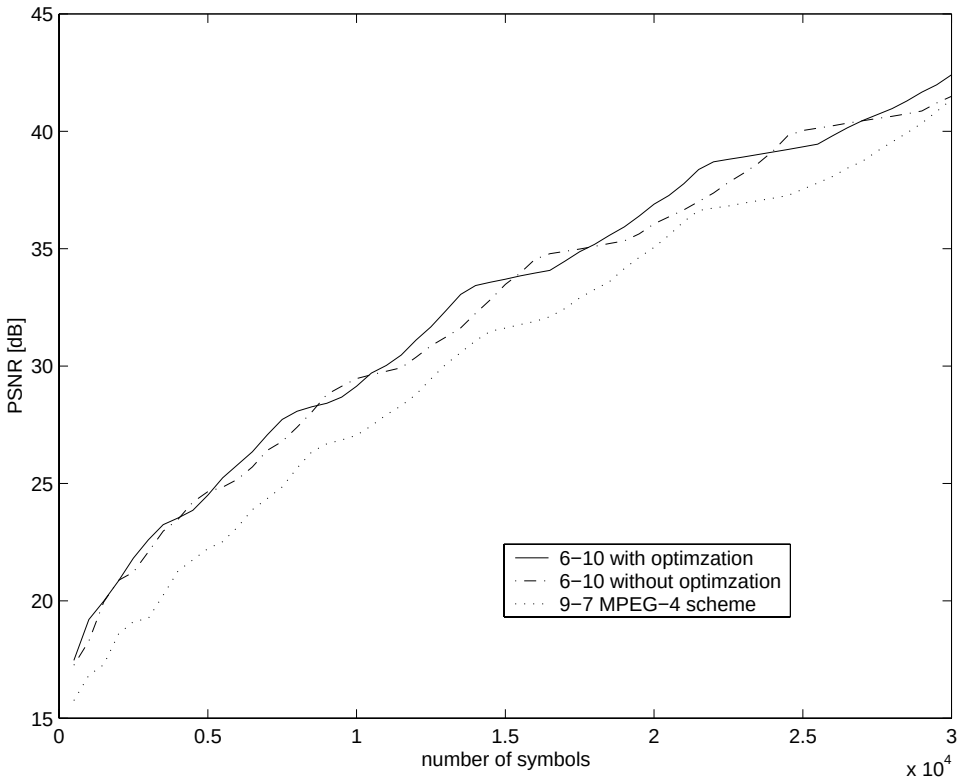

Figure 9. Rate-distortion results for the cameraman foreground. The rate is measured in terms of the number of symbols coded by the SA EZW coder.

level, the shape of the LL band becomes more and more regular than for other SA DWTs, the loss due to irregular shapes decreases, and the compaction gain increases. The proposed decomposition is especially advantageous when the DWT coefficients are to be compressed via embedded zerotree coding.

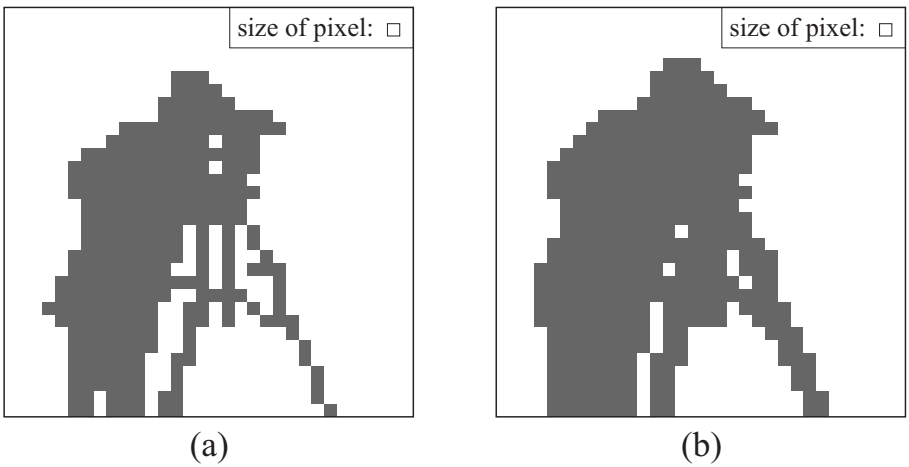

Figure 10. Shape of LL band of decomposed cameraman image at third decomposition level. (a) MPEG-4 scheme; (b) proposed scheme.

REFERENCES

1. M. Gilge, Region-oriented texture coding. In *Video Coding – The Second Generation Approach,* L. Torres and M. Kunt (eds.), pp. 171–218. Kluwer, 1996.
2. T. Sikora and B. Makai, "Shape-adaptive DCT for generic coding of video," *IEEE Trans. Circ. and Syst. for Video Technology* **5**, pp. 59–62, Feb. 1995.
3. "MPEG-4 Video Verification Model, Version 14. Generic Coding of Moving Pictures and Associated Audio, ISO/IEC JTC1/SC 29/WG 11," 1999.
4. H. J. Barnard, J. H. Weber, and J. Biemond, A Region-Based Discrete Wavelet Transform for Image Coding. In *Advances in Image Communication: Wavelets in Image Communication,* M. Barlaud (ed.), vol. 5, pp. 189–227. Elsevier, Amsterdam, 1994.
5. J. R. Casas and L. Torres, "A region-based subband coding scheme," *Signal Processing: Image Communications* **10**, pp. 173–200, 1997.
6. J. Li and S. Lei, "Shape adaptive wavelet transform with phase alignment," in *Proc. IEEE ICIP'98*, vol. 3, pp. 683–687, (Chicago), Oct. 1998.
7. S. Li and W. Li, "Shape adaptive discrete wavelet transform for coding arbitrarily shaped texture," in *Proc. SPIE, VCIP, San Jose, CA*, vol. 3024, pp. 1046–1056, Jan. 1997.
8. H. Katata, N. Ito, T. Anno, and H. Kusao, "Object wavelet transform for coding of arbitrarily shaped image segments," *IEEE Trans. Circ. and Syst. for Video Technology* **7**, pp. 234–237, Feb. 1997.
9. J. D. Villasenor, B. Belzer, and J. Liao, "Wavelet filter evaluation for image compression," *IEEE Trans. Image Processing* **4**, pp. 1053–1060, Aug. 1995.
10. A. Mertins, "Optimized biorthogonal shape adaptive wavelets," in *Proc. IEEE Int. Conf. Image Processing*, vol. 3, pp. 673–677, (Chicago), Oct. 1998.
11. J. Woods and S. O'Neil, "Subband coding of images," *IEEE Trans. Acoust., Speech, Signal Processing* **34**, pp. 1278–1288, May 1986.
12. M. J. T. Smith and S. L. Eddins, "Analysis/synthesis techniques for subband coding," *IEEE Trans. Acoust., Speech, Signal Processing* , pp. 1446–1456, Aug. 1990.
13. H. J. Barnard, J. H. Weber, and J. Biemond, "Efficient signal extension for subband/wavelet decomposition of arbitrary length signals," in *Proc. SPIE, VCIP*, vol. 2094, pp. 966–975, Nov. 1993.
14. L. Chen, T. Q. Nguyen, and K. P. Chan, "Symmetric extension methods for M-channel linear-phase perfect reconstruction filter banks," *IEEE Trans. Signal Processing* **SP-43**, pp. 2505–2511, Nov. 1995.
15. J. N. Bradley, C. M. Brislawn, and V. Faber, "Reflected boundary conditions for multirate filter banks," in *Proc. Int. Symp. Time-Frequency and Time-Scale Analysis*, pp. 307–310, (Canada), 1992.

16. R. L. de Queiroz, "Subband processing of finite length signals without border distortions," in *Proc. IEEE Int. Conf. Acoust., Speech, Signal Processing*, vol. IV, pp. 613 – 616, (San Francisco, USA), Mar. 1992.
17. C. Herley, "Boundary filters for finite-length signals and time-varying filter banks," *IEEE Trans. Circuits and Systems II* **42**, pp. 102–114, Feb. 1995.
18. A. Mertins, "Image compression via edge-based wavelet transform," *Optical Engineering* **38**, pp. 991–1000, June 1999.
19. V. Nuri and R. H. Bamberger, "Size limited filter banks for subband image compression," *IEEE Trans. Image Processing* **4**, pp. 1317–1323, Sept. 1995.
20. J. M. Shapiro, "Embedded image coding using zerotrees of wavelet coefficients," *IEEE Trans. Signal Processing* **41**, pp. 3445–3462, Dec. 1993.
21. A. Said and W. A. Pearlman, "A new fast and efficient image codec based on set partitioning in hierarchical trees," *IEEE Trans. Circ. and Syst. for Video Technology* **6**, pp. 243–250, June 1996.